

# 1

## Introduction

Uchida [1], who suggested the idea of plasma and magnetic field diagnostics in the solar corona on the basis of waves and oscillations in 1970, and Rosenberg [2], who first explained the pulsations in type IV solar radio bursts in terms of the loop magnetohydrodynamic (MHD) oscillations, can be considered to be pioneers of coronal seismology.

Various approaches have been used to describe physical processes in stellar coronal structures: kinetic, MHD, and electric circuit models are among them. Two main models are presently very popular in coronal seismology. The first considers magnetic flux tubes and loops as wave guides and resonators for MHD waves and oscillations, whereas the second describes a loop in terms of an equivalent electric (RLC) circuit. Several detailed reviews are devoted to problems of coronal seismology (see, i.e., [3–7]). Recent achievements in the solar coronal seismology are also referred in *Space Sci. Rev.* vol. 149, No. 1–4 (2009). Nevertheless, some important issues related to diagnostics of physical processes and plasma parameters in solar and stellar flares are still insufficiently presented in the literature. The main goal of the book is the successive description and analysis of the main achievements and problems of coronal seismology.

There is much in common between flares on the Sun and on late-type stars, especially red dwarfs [8]. Indeed, the timescales, the Neupert effect, the fine structure of the optical, radio, and X-ray emission, and the pulsations are similar for both solar and stellar flares. Studies of many hundreds of stellar flares have indicated that the latter display a power-law radiation energy distribution, similar to that found for solar flares. Thus, we can use the solar–stellar analogy to study flaring stars.

The next goal of this book is to illustrate the efficiency of coronal seismology as a diagnostic tool for the analysis of stellar flares.

### 1.1

#### **Magnetic Loops and Open Flux Tubes as Basic Structural Elements in Solar and Stellar Coronae**

Magnetic loops constitute the basic structural element in the coronae of the Sun and late-type stars [9–11]. They play an important role in solar activity. Observations

made with *Skylab*, Solar and Heliospheric Observatory (SOHO), *Yohkoh*, Reuven Ramaty High-Energy Solar Spectroscopic Imager (RHESSI), Transition Region and Coronal Explorer (TRACE), Complex Orbital Near-Earth Observations of Activity of the Sun – Photon (CORONAS–F), *Hinode*, Solar Dynamic Observatory (SDO) space missions, as well as with large optical telescopes Vacuum Tower Telescope (VTT), and radio telescopes (Very Large Array (VLA), Siberian Solar Radio Telescope (SSRT), NoRH (Nobeyama Radioheliograph)) have shown that solar flares originate in coronal loops [3, 12]. Eruptive prominences and coronal transients result in giant coronal mass ejections (CMEs) and also frequently display the loop shape [13]. The flaring activity of dMe-stars and close binaries is also spawned by the energy release in magnetic loops [9, 14, 15]. In some late-type stars, magnetic spots cover up to 70–80% of the surface, whereas solar spots occupy  $\sim 0.04\%$  of the photosphere. This implies that, in fact, loops form the magnetic structure of stellar coronae. In addition, loops are typical for the magnetic structure of the atmospheres of accretion disks, young stellar objects, and neutron stars [16–19]. Owing to space-borne observations and advances in the physics of the loops, some progress has been recently made in finding a solution for the problem of the origin of coronal loops. Alfvén and Carlqvist [20] have suggested that a flaring loop can be considered to be an equivalent electric circuit. This phenomenological approach was nevertheless very productive in understanding the energy pattern of flare processes. The description of the loops in terms of resonators and wave guides for MHD waves explains various kinds of modulations of stellar flare emissions and serves as a diagnostic tool for the flare plasma. The concept of a coronal loop as a magnetic mirror trap for energetic particles makes it possible to efficiently describe particle dynamics and peculiarities of emission generated by energetic particles.

Open magnetic structures – the flux tubes – are wave guides for MHD waves, which make them important channels of energy transfer from one part of the stellar atmosphere to another, from the photosphere and chromosphere to the corona, and further to the solar and stellar wind. Similar to magnetic loops, the flux tubes provide a necessary link in the mechanism of coronal heating. Flux tubes are exemplified by solar spicules, which are energy/mass bridges between the dense and dynamic photosphere and the tenuous hot solar corona [21].

Prominence dynamics and oscillations also present important subjects for coronal seismology [22, 23] since prominences play a crucial role both in triggering flares [24, 25] and in CME's origin [26]. Therefore, the study of ballooning instability presents a very important point in the context of flaring and CME's activity.

## 1.2

### Data of Observations and Types of Coronal Loops

The corona of the Sun (a main-sequence G2 star) in its active phase consists predominantly of magnetic loops filled with comparatively dense and hot plasma, which is observed in soft X rays and constitutes an essential part of the total mass of the corona. The presence of magnetic loops indicates the complexity

of the subphotospheric magnetic field, which is most likely linked to convective motions of the photosphere matter. Observations indicate that there are at least five morphologically distinct types of loops present in the solar atmosphere (see, i.e., [27, 28]):

- 1) **Loops connecting different active regions.** Their lengths reach 700 000 km, the plasma temperature in such loops is  $(2-3) \times 10^6$  K, and the density is about  $10^9 \text{ cm}^{-3}$ . The loop footpoints are located in islands of the strong magnetic field on the periphery of active regions. The characteristic lifetime of such loops is about one day.
- 2) **Loops in quiescent regions.** They do not connect active regions; their lengths are the same as those of the previous types of loops. Their temperature, however, is somewhat lower, within the interval  $(1.5-2.1) \times 10^6$  K, while the density is in the range  $(2-10) \times 10^8 \text{ cm}^{-3}$ .
- 3) **Loops in active regions.** Their lengths span from 10 000 to 100 000 km and temperature and density are within the intervals  $10^4-2.5 \times 10^6$  K and  $(0.5-5.0) \times 10^9 \text{ cm}^{-3}$ , respectively.
- 4) **Post-flare loops.** They commonly connect footpoints of two-ribbon flares, and display lengths of 10 000–100 000 km, temperature  $10^4-4 \times 10^6$  K, and density up to  $10^{11} \text{ cm}^{-3}$ .
- 5) **Single-flare loops.** These are separate loops, in which flare energy is released. Hard X-ray bursts last for about a minute and are the most pertinent feature of such flares. In soft X rays, these loops are characterized by small volumes and low heights. The loops are 5000–50 000 km in length, their temperature is less than  $4 \times 10^7$  K, and their plasma density reaches  $10^{12} \text{ cm}^{-3}$  [12].

Closed magnetic structures resembling coronal loops also exist in stars of other types. Data obtained with *Einstein*, *ROSAT* (Röntgensatellit), and *XMM-Newton* (XMM stands for X-ray multimirror mission) space missions indicate that virtually all stars on the Hertzsprung–Russel diagram possess hot coronae with temperatures ranging between  $10^7$  and  $10^8$  K [29–31]. They are not confined gravitationally, which implies the presence of magnetic fields. Of special interest are late-type stars, particularly dMe red dwarfs, which display high flare activity and represent nearly 80% of the total number of stars in the Galaxy and in its close neighborhood. Although red dwarfs are morphologically similar to the Sun, especially in their radio-wavelength radiation (the slowly varying component, rapidly drifting bursts, sudden reductions, spike bursts, and quasi-periodical pulsations [15, 32]), these objects present some peculiarities, which stem from the high activity of their coronae.

First, note the high brightness temperature of the “quiescent” radio emission of dMe-stars (up to  $10^{10}$  K), which cannot be described in terms of thermal coronal plasma with the temperature  $10^7-10^8$  K. This radiation is commonly interpreted as gyrosynchrotron emission of nonthermal electrons abundant in the coronae of red dwarfs. The coexistence of the hot plasma and subrelativistic particles is also suggested by the correlation between the radio and soft X-ray emission over six orders of magnitude in intensity [33]. This phenomenon is not observed in the solar corona. In the quiescent state, the corona of the Sun does not host a sufficient

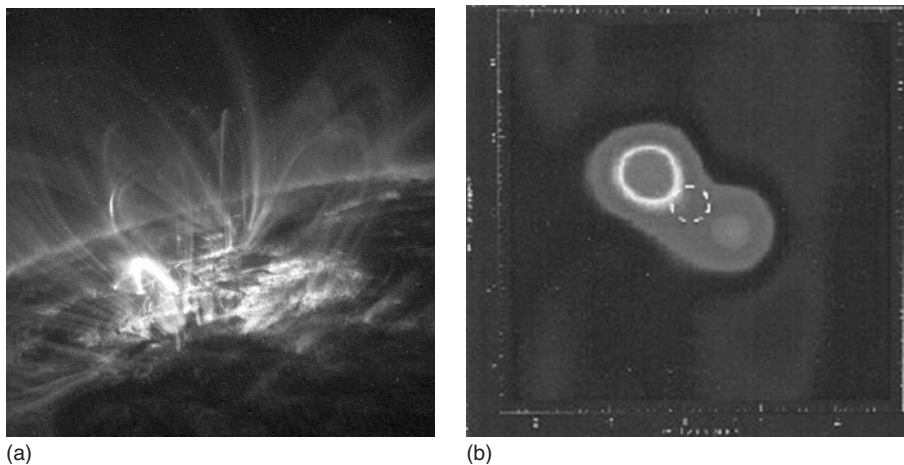


**Figure 1.1** (a) Coronal magnetic loops of an active region on the Sun observed with the space laboratory TRACE in the ultraviolet range,  $\lambda = 171 \text{ \AA}$  [11]. A hot flare loop stands out sharply. (b) Radio map of UV Cet on the wavelength of 3.6 cm obtained with VLBA (very long baseline array) and VLA (very large array). The dashed line marks the optical disk of the star [10].

**Table 1.1** Parameters of coronal flare loops.

Parameter	The Sun	Red dwarf UV Ceti	Close binary stars	
			RS CVn	Algol
Length (cm)	$(1-10) \times 10^9$	$2 \times 10^9 - 3 \times 10^{11}$	$(5-10) \times 10^{10}$	$(2-6) \times 10^{11}$
Lateral size (cm)	$(1-5) \times 10^8$	$10^8 - 3 \times 10^9$	—	—
Plasma density $n$ ( $\text{cm}^{-3}$ )	$10^9 - 10^{12}$	$10^{10} - 10^{12}$	$10^8 - 10^{10}$	$10^9 - 10^{12}$
Plasma temperature $T$ (K)	$10^6 - 10^7$	$3 \times 10^6 - 10^8$	$(3-9) \times 10^7$	$(3-7) \times 10^7$
Magnetic field induction $B$ (G)	$10^2 - 10^3$	$3 \times 10^2 - 10^3$	$(0.3-6) \times 10^2$	$(1-5) \times 10^2$
Emission measure (EM) ( $\text{cm}^{-3}$ )	$10^{47} - 10^{50}$	$10^{50} - 10^{53}$	$10^{53} - 10^{55}$	$10^{52} - 10^{54}$

number of high-energy particles, and the brightness temperature of solar radio emission does not exceed  $10^6$  K.

Second, the difference is manifested in the extremely high brightness temperature of flare radio emission of red dwarves, sometimes exceeding  $10^{16}$  K, which is three to four orders of magnitude higher than that of the most powerful radio bursts in the Sun. This suggests the presence of an efficient coherent (maser) mechanism of emission from stellar coronae. Moreover, in red dwarfs, radio flares can frequently occur independently of optical flares.

Third, the sizes of loops on the Sun and red dwarves are different [9, 10]. As a rule, the length of the solar loops, with the exception of trans-equatorial ones, is substantially smaller than that of the solar radius (Figure 1.1a). On red dwarves, the size of magnetic loops can be comparable to the stellar radii or can exceed them by a few factors (Figure 1.1b). The magnetic field in stellar loops can exceed that in solar loops by an order of magnitude.

Table 1.1 presents parameters of flare loops on the Sun and late-type stars derived from multiwavelength (optical, radio, and X-ray) observations and various diagnostic methods.

### 1.3 The MHD Approach for Coronal Plasma

In our study of magnetic structures in coronal plasma and their evolution, we frequently use MHD approximation. It includes Maxwell equations, generalized Ohm's law, and also equations of motion and continuity of mass, the energy equation, and the gas equation of state. In MHD approximation, it is common to take the simplified Maxwell equations, without taking into account the bias current, and also the simplified form of the Ohm's law in the approximation of isotropic conductivity of plasma. For a number of problems of coronal seismology, such approximations appear to be insufficient, and more general equations are used. In addition to that, when the dynamics and radiation of fast particles in coronal magnetic loops are analyzed, the kinetic equation for the velocity distribution of particles should be used (see, for example, Chapters 6 and 7). Below, we present the basic equations of magnetic hydrodynamics in their generalized form, which is applied further on. For the sake of convenience, we repeatedly reproduce these equations along with the explanation for the previously used notation in different sections.

The *Maxwell equations* in the Gaussian system of units (cgs) may be written in the form

$$\text{rot} \vec{B} = \frac{4\pi}{c} \mu \vec{j} + \frac{1}{c} \mu \varepsilon \frac{\partial \vec{E}}{\partial t} \quad (1.1)$$

$$\text{rot} \vec{E} = -\frac{1}{c} \frac{\partial \vec{B}}{\partial t} \quad (1.2)$$

$$\text{div} \vec{B} = 0 \quad (1.3)$$

$$\text{div} \vec{E} = \frac{1}{\varepsilon} 4\pi \rho_e \quad (1.4)$$

Here, the magnetic induction  $\vec{B}$  and magnetic field  $\vec{H}$  are related as follows:  $\vec{B} = \mu \vec{H}$ , while the electric field  $\vec{E}$  may be expressed through electric induction:  $\vec{E} = \vec{D}/\varepsilon$ , where  $\mu$  and  $\varepsilon$  are magnetic and dielectric permeabilities. For coronal plasma,  $\mu$  and  $\varepsilon$  are usually taken to be equal to their values in vacuum; in the Gaussian system of units (cgs), we further assume  $\mu = \varepsilon = 1$ . In Eqs. (1.1)

and (1.4),  $\vec{j}$  and  $\rho_e$  are the density of the electric current and electric charge, respectively.

The *generalized Ohm's law* follows the “three-fluid” model for electrons, ions, and neutral atoms; it connects the electric current with the velocity of the center of mass, and also with the electric and magnetic fields. When the inertia of electrons is neglected, the generalized Ohm's law is written as follows:

$$\vec{E} + \frac{1}{c} \vec{V} \times \vec{B} = \frac{\vec{j}}{\sigma} + \frac{\vec{j} \times \vec{B}}{enc} + \frac{\vec{f}_e}{en} + F \frac{[\vec{f}_a \times \vec{B}]}{cnm_i v'_{ia}} - \frac{F^2 \rho}{cnm_i v'_{ia}} \left[ \frac{d\vec{V}}{dt} \times \vec{B} \right] \quad (1.5)$$

Here,  $\rho = n_a m_a + n_e m_e + n_i m_i$  is the plasma density,  $p = p_a + p_e + p_i$  is its pressure,  $\vec{V} = \left( \sum_k n_k m_k \vec{V}_k \right) / \left( \sum_k n_k m_k \right)$  is the average velocity of plasma motion,  $k = a, i, e$  (a, atoms; i, ions; and e, electrons),  $\sigma = \frac{ne^2}{m_e(v'_{ei} + v'_{ea})}$  is the Coulomb (Spitzer) conductivity,  $F = \rho_a / \rho$  is the relative density of neutrals,  $\nu_{kl}$  is the frequency of collisions between particles of  $k$  and  $l$  types,  $\nu'_{kl} = [m_l / (m_k + m_l)] \nu_{kl}$  is the effective frequency of collisions,  $n_i = n_e = n$ ,  $\vec{f}_e = -\text{grad } p_e$ ,  $\vec{f}_a = -\text{grad } p_a + n_a m_a \vec{g}$ , and  $\vec{g}$  is the gravitational acceleration. Two last summands in the right-hand part of Eq. (1.5) take into account dissipation related to ion–atom collisions. Under the conditions in the chromospheres and even of the corona, this dissipation frequently appears to be more efficient than that caused by Spitzer conductivity  $\sigma$ .

*The induction equation.* Excluding the electric field from Eq. (1.5) with the use of Eq. (1.2), we obtain the following equation for magnetic induction:

$$\begin{aligned} \frac{\partial \vec{B}}{\partial t} &= \eta \nabla^2 \vec{B} + \text{rot} [\vec{V} \times \vec{B}] + \frac{F^2 \rho}{n_i m_i v'_{ia}} \text{rot} \left[ \frac{d\vec{V}}{dt} \times \vec{B} \right] \\ &\quad - \frac{F}{n_i m_i v'_{ia}} \text{rot} [\vec{f}_a \times \vec{B}] - \frac{1}{en_i} \text{rot} [\vec{j} \times \vec{B}] \end{aligned} \quad (1.6)$$

where  $\eta = c^2 / 4\pi \sigma$  is the magnetic viscosity. Frequently, only the first two terms in the right-hand part of the induction Eq. (1.6) are taken into account, which correspond to the simplest form of the Ohm's law

$$\vec{j} = \sigma \left( \vec{E} + \frac{1}{c} \vec{V} \times \vec{B} \right) \quad (1.5a)$$

This form of Ohm's law may be applied, for instance, in the case of totally ionized plasma ( $\vec{f}_a = 0$ ), provided the Ampere force becomes zero ( $\vec{j} \times \vec{B} = 0$ , the so-called force-free approximation). In a more general case, for example, in the lower chromosphere or in the prominence, plasma is partly ionized, and the anisotropy of conductivity becomes essential. Therefore, the more general induction Eq. (1.6) should be used.

*Equations of plasma.* The induction Eq. (1.6) indicates that the behavior of the magnetic field is related to the motion of plasma, since in this equation some summands contain the matter velocity. In turn, the motion of plasma is specified

by the continuity equation, the equation of motion, and the energy equation:

$$\frac{\partial \rho}{\partial t} + \text{div}(\rho \vec{V}) = 0 \quad (1.7)$$

$$\rho \frac{D\vec{V}}{Dt} = -\nabla p + \frac{1}{c} \vec{j} \times \vec{B} + \rho \vec{g} \quad (1.8)$$

$$\frac{\rho^\gamma}{\gamma - 1} \frac{D}{Dt} \left( \frac{p}{\rho^\gamma} \right) = -Q \quad (1.9)$$

In Eqs. (1.8) and (1.9),  $D/Dt = \partial/\partial t + (\vec{v}\nabla)$  means the convective derivative that specifies time variations of parameters related to plasma motion. In Eq. (1.9),  $\gamma = C_P/C_V$  is the ratio between specific heat capacities and  $Q$  is the function equal to the difference between the energy loss and energy inflow rates per unit volume of plasma. The energy loss commonly consists of the thermal conductivity and radiative losses. In coronal magnetic fields, the thermal conductivity across the magnetic field may commonly be neglected. In addition to that, in the optically thin part of the atmosphere ( $T \geq 2 \times 10^4$  K in the chromosphere and in the corona), the radiative losses do not depend on the radiation intensity, which results in simplification of the radiative loss function. If along with that the energy inflow rate is specified by dissipation of electric currents, the function  $Q$  may be presented as follows:

$$Q = -\frac{1}{A} \frac{d}{ds} \left( \kappa_e \frac{dT}{ds} A \right) + n_e n_H \chi(T) - \left( \vec{E} + \frac{1}{c} \vec{V} \times \vec{B} \right) \vec{j} \quad (1.10)$$

Here,  $A(s)$  is the cross section of the force tube related to the magnetic field,  $s$  is the coordinate along the tube, and  $\kappa_e = 0.92 \times 10^{-6} \text{ erg cm}^{-1} \text{ K}^{-7/2}$  is the coefficient of thermal conductivity along the magnetic field,

$$\begin{aligned} \chi(T) &\approx 10^{-21.85} \quad (10^{4.3} \leq T \leq 10^{4.6} \text{ K}) \\ &\approx 10^{-31} T^2 \quad (10^{4.6} \leq T \leq 10^{4.9} \text{ K}), \\ &\approx 10^{21.2} \quad (10^{4.9} \leq T \leq 10^{5.4} \text{ K}) \\ &\approx 10^{-10.4} T^{-2} \quad (10^{5.4} \leq T \leq 10^{5.75} \text{ K}) \\ &\approx 10^{-21.94} \quad (10^{5.75} \leq T \leq 10^{6.3} \text{ K}) \\ &\approx 10^{-17.73} T^{-2/3} \quad (10^{6.3} \leq T \leq 10^7 \text{ K}) \end{aligned} \quad (1.11)$$

is the temperature function, the values of which are presented, for example, in Ref. [34];  $n_H$  is the number of hydrogen atoms in the unit volume (for totally ionized plasma,  $n_H = n_e$ ). The last summand in Eq. (1.10) is determined by taking Ohm's law into account (Eq. (1.5)). Within the temperature interval  $10^5 \text{ K} < T < 10^7 \text{ K}$ , a possible approximation for the radiative loss function is  $\chi(T) = \chi_0 T^{-1/2} \text{ erg cm}^3 \text{ s}^{-1}$ , where  $\chi_0 = 10^{-19}$  [27].

The connection between the pressure and the density is specified by the equation of state; for ideal gas,

$$p = nk_B T \quad (1.12)$$

where  $n = n_e + n_i + n_a$  is the total number of particles in unit volume and  $k_B$  is the Boltzmann's constant. Different versions of the equations used in MHD approximation are considered in more detail in the monograph by Priest [27].

## References

1. Uchida, Y. (1970) *Publ. Astron. Soc. Jpn.*, **22**, 341.
2. Rosenberg, H. (1970) *Astron. Astrophys.*, **9**, 159.
3. Aschwanden, M.J., Poland, A.I., and Rabin, D. (2001) *Ann. Rev. Astron. Astrophys.*, **39**, 175.
4. Aschwanden, M.J. (2003) NATO Advances Research Workshop, NATO Science Series II, p. 22.
5. Nakariakov, V.M. and Verwichte, E. (2005) *Living Rev. Sol. Phys.* Coronal waves and oscillations, **2**, No 3, pp. 3–65
6. Nakariakov, V.M. and Stepanov, A.V. (2007) *Lect. Notes Phys.*, **725**, 221.
7. Zaitsev, V.V. and Stepanov, A.V. (2008) *Phys. Usp.*, **51**, 1123.
8. Gershberg, R.E. (2005) *Solar-Type Activity in Main-Sequence Stars*, Springer, Berlin, Heidelberg.
9. Bray, R.J., Cram, L.E., Durrant, C.J., and Loughhead, R.E. (1991) *Plasma Loops in the Solar Corona*, Cambridge University Press.
10. Benz, A., Conway, J., and Güdel, M. (1998) *Astron. Astrophys.*, **331**, 596.
11. Schrijver, C.J., Title, A.M., Berger, T.E., Fletcher, L. *et al.* (1999) *Sol. Phys.*, **187**, 261.
12. Sakai, J.-I. and de Jager, C. (1996) *Space Sci. Rev.*, **77**, 1.
13. Plunkett, S.P., Vourlidas, A., Šimberová, S., Karlický, M. *et al.* (2000) *Sol. Phys.*, **194**, 371.
14. Lestrade, J.F. (1988) *Astrophys.J.*, **328**, 232.
15. Bastian, T.S., Bookbinder, J.A., Dulk, G.A., and Davis, M. (1990) *Astrophys.J.*, **353**, 265.
16. Galeev, A.A., Rosner, R., Serio, S., and Vaiana, G.S. (1981) *Astrophys.J.*, **243**, 301.
17. Kuijpers, J. (1995) *Lect. Notes Phys.*, **444**, 135.
18. Feigelson, E.D. and Montmerle, T. (1999) *Ann. Rev. Astron. Astrophys.*, **37**, 363.
19. Beloborodov, A.M. and Thompson, C. (2007) *Astrophys.J.*, **657**, 967.
20. Alfvén, H. and Carlqvist, P. (1967) *Sol. Phys.*, **1**, 220.
21. Zaqarashvili, T.V. and Erdelyi, R. (2009) *Space Sci. Rev.*, **149**, 355.
22. Oliver, R. (2009) *Space Sci. Rev.*, **149**, 175.
23. Tripathi, D., Isobe, H., and Jain, R. (2009) *Space Sci. Rev.*, **149**, 283.
24. Pustyl'nik, L.A. (1974) *Sov. Astron.*, **17**, 763.
25. Zaitsev, V.V., Urpo, S., and Stepanov, A.V. (2000) *Astron. Astrophys.*, **357**, 1105.
26. Gopalswamy, N. (2006) *Space Sci. Rev.*, **124**, 145.
27. Priest, E.R. (1982) *Solar Magnetohydrodynamics*, D. Reidel Publishing Company, Dordrecht.
28. Aschwanden, M.J. (2005) *Physics of the Solar Corona. An Introduction with Problems and Solutions*, Springer.
29. Haisch, B.M. (1983) in *Activity in Red-Dwarf Stars X-ray Oscillations of Stellar Flares* (eds P.B. Birne and M. Rodono), Reidel, p. 255–268.
30. Schmitt, J.H.M.M., Collura, A., Sciortino, S., Vaiana, G.S. *et al.* (1990) *Astrophys.J.*, **365**, 704.
31. Mullan, D.J., Mathioudakis, M., Bloomfield, D.S., and Christian, D.J. (2006) *Astrophys.J. Suppl.*, **164**, 173.
32. Stepanov, A.V., Kliem, B., Zaitsev, V.V. *et al.* (2001) *Astron. Astrophys.*, **374**, 1072.
33. Güdel, M. and Benz, A.O. (1993) *Astrophys.J.*, **405**, L63.
34. Rosner, R., Tucker, G.S., and Vaiana, R. (1978) *Astrophys.J.*, **220**, 643.